



# Multiscale fatigue damage characterization in short glass fiber reinforced polyamide-66



M.F. Arif<sup>a</sup>, N. Saintier<sup>b,\*</sup>, F. Meraghni<sup>a</sup>, J. Fitoussi<sup>c</sup>, Y. Chemisky<sup>a</sup>, G. Robert<sup>d</sup>

<sup>a</sup> Arts et Métiers ParisTech, LEM3 – UMR CNRS 7239, 4 Rue Augustin Fresnel, 57078 Metz, France

<sup>b</sup> Arts et Métiers ParisTech, I2M – UMR CNRS 5295, Esplanade des Arts et Métiers, 33405 Talence, France

<sup>c</sup> Arts et Métiers ParisTech, PIMM – UMR CNRS 8006, 151 Boulevard de l'Hôpital, 75013 Paris, France

<sup>d</sup> Solvay Engineering Plastics, Avenue Ramboz BP 64, 69192 Saint-Fons, France

## ARTICLE INFO

### Article history:

Received 13 August 2013

Received in revised form 30 November 2013

Accepted 9 January 2014

Available online 18 January 2014

### Keywords:

A: Polymer–matrix composites (PMCs)

B: Fatigue

B: Microstructures

E: Injection molding

Micro-computed tomography

## ABSTRACT

This paper aims at studying fatigue damage behavior of injection molded 30 wt% short glass fiber reinforced polyamide-66 composite (PA66/GF30). The evolution of dynamic modulus, hysteresis area, cyclic creep and temperature during fatigue tests were analyzed and discussed. Damage analyses by X-ray micro-computed tomography ( $\mu$ CT) technique on interrupted fatigue tests at several percentages of total fatigue life were performed to further understand the damage mechanisms and evolution during fatigue loading. It can be observed that experimental results related to the evolution of dynamic modulus, strain, temperature and energy dissipation are important and consistently complement each other for damage evaluation of PA66/GF30. During fatigue loading, diffuse damage occurs over the entire specimen though the damage does not necessarily exhibit the same level between different locations inside the specimen. The  $\mu$ CT analysis of voids characteristics demonstrates that the damage continuously increases during fatigue loading. The damage is developed notably along fiber interface in the form of fiber/matrix interfacial debonding.

© 2014 Elsevier Ltd. All rights reserved.

## 1. Introduction

The reduction of vehicle mass is a major concern for automotive industries to comply with the strict pollution regulation, particularly for the CO<sub>2</sub> emission. Short fiber reinforced thermoplastic materials, among them is the short glass fiber reinforced polyamide-66, are good candidates to provide a compromise between the required lightweight and the expected thermomechanical performances. However, their structural durability has not yet been fully investigated. In particular further work to investigate the fatigue behavior of these composites is necessary to provide physically based damage mechanisms scenarios for fatigue modeling.

Various techniques have been used to evaluate the damage in short fiber reinforced thermoplastics. Early works of Horst and Spoormaker [1,2] performed fractography analysis onto the fracture surface of fatigue loaded short glass fiber reinforced polyamides by scanning electron microscopy (SEM) and they proposed a damage mechanisms scenario which consider that the damage starts at fiber ends and then propagates along fiber interface. The evolution of dynamic modulus, i.e. the slope of stress–strain hys-

teresis curve, has been proposed by several authors to evaluate the damage level of the composites [3–8]. Since the damage process is thermally activated and, in the same time, a dissipative process by nature, thermography technique by using infra-red camera has become an important tool for fatigue damage evaluation in composites [9–14]. Finally, due to the complex nature of the microstructure, damage is spatially distributed so that X-ray micro-computed tomography ( $\mu$ CT) technique has become a suitable and efficient tool for fatigue damage characterization in composite materials [15–17]. The work of Cosmi and Bernasconi [18] presents the potential and critical aspects of using  $\mu$ CT technique for fatigue damage characterization in short glass fiber reinforced polyamides. The current work is the continuation of the recently published work on damage characterization of PA66/GF30 under quasi-static loading by SEM and  $\mu$ CT techniques [19].

During fatigue loading of the composite, several phenomena may develop concurrently, such as damage, cyclic creep and increase of temperature. All of them may contribute to the overall fatigue strength of the material [20,21]. A comprehensive study of fatigue damage behavior is necessarily a coupled analysis of all interrelating phenomena during fatigue loading. The objective of this work is to characterize fatigue damage mechanisms of PA66/GF30 under uniaxial constant amplitude loading. It is proposed

\* Corresponding author. Tel.: +33 556 845 361; fax: +33 556 845 366.

E-mail address: [nicolas.saintier@ensam.eu](mailto:nicolas.saintier@ensam.eu) (N. Saintier).

to use a combined analysis of dynamic modulus, cyclic creep, dissipated energy and temperature evolution during fatigue testing together with post-mortem 3D damage analysis by  $\mu$ CT to further understand the damage mechanisms of PA66/GF30 during fatigue testing. To evaluate the process induced anisotropy, two directions, longitudinal and transverse to the mold flow direction (MFD), are examined. In addition, a particular attention is given to the effect of skin-shell-core formation on the damage mechanisms of PA66/GF30. In fact, this type of microstructure is commonly observed in the injection molded short glass fiber reinforced polyamides [22–25]. The experimental results allow to analyze the importance of damage and their interrelated phenomena to the overall behavior of PA66/GF30, as well as to the identification of damage mechanisms and evolution.

In summary, the organization of this work is as follows: Section 2 presents material and process induced microstructure description, followed by the specimens used for mechanical characterization in Section 3. In Section 4, the experimental procedures and damage investigation techniques are detailed. In Section 5, the results of microscopic and macroscopic damage analysis of PA66/GF30 are discussed. Afterwards, the damage characteristics and all the contributing factors to the overall fatigue strength, as well as the damage mechanisms chronology of PA66/GF30 are concluded in Section 6.

## 2. Material and process induced microstructure description

The material studied is a 30 wt% short glass fiber reinforced polyamide-66 composite (PA66/GF30) provided by Solvay Engineering Plastics-France, under the commercial name of Technyl® A218V30. The material was prepared by compounding the polyamide-66 pellets and chopped short glass fibers in a twin-screw extruder. Subsequently, PA66/GF30 compound was transferred into an injection molding machine, resulting in  $360 \times 100 \times 3.2$  mm<sup>3</sup> of rectangular plate.

It is commonly established through open literature [22–25] that fiber orientation distribution is widely governed by injection process. In fact, for a system where polymer melt flows through a small cavity between two parallel walls, shear flow has maximum value near to the mold wall whereas it vanishes at the core zone. This leads the fibers to be oriented parallel (and perpendicular) to MFD at the shell (and core) layers. Moreover, a thin random skin layer can be formed due to the polymer melt that is in direct contact with a relatively cold mold wall temperature.

X-ray micro-computed tomography ( $\mu$ CT) technique was employed to study the microstructure heterogeneity of PA66/GF30 in terms of its fiber orientation. The  $\mu$ CT experiment was carried out at ID19 beam line of the European Synchrotron Radiation Facility (ESRF) Grenoble, France [26]. For this microstructure investigation, the experimental setup was conditioned to reach a voxel resolution of 1.4  $\mu$ m. Two samples for  $\mu$ CT experiments were extracted from the injection molding plate at two positions along mold flow direction (MFD) axis, as shown in Fig. 1. The selected positions were significantly far from the complex flow zones at

the initial and final filling stages. Indeed, nonuniform microstructure is usually found at these complex flow zones. Moreover, the selected positions were also used as a guideline for specimens extraction for the tensile and fatigue tests that will be discussed in Section 3. The dimensions of the  $\mu$ CT samples were  $2 \times 2 \times 3.2$  mm<sup>3</sup>, where 3.2 mm corresponds to the sample thickness. The  $\mu$ CT scanning was not carried out through all the sample thickness but it always covered more than half of the thickness so that the skin-shell-core structure can always be captured.

The microstructure of PA66/GF30 obtained from the  $\mu$ CT sample extracted from position A of Fig. 1 is shown in Fig. 2. It can be seen from Fig. 2, PA66/GF30 has a specific injection molding process induced microstructure characterized by a skin-shell-core structure. Moreover, transition layers between shell and core are also observed. The microstructure of PA66/GF30 extracted from position B exhibits qualitatively the same trend as the one extracted from position A. This microscopic condition was achieved by an optimal set up of injection molding parameters (barrel and mold temperatures, injection speed, etc.) to ensure a high compaction degree of PA66/GF30 and to reduce the core layer thickness.

To acquire the real tendency of fiber orientation throughout the samples, the tensor representation of fiber orientation state proposed by Advani and Tucker [27] is used in this work. This method is widely used to characterize the fiber orientation due to its efficiency, simplicity and relatively short computational time. The complete review of this method can be found elsewhere [28–30]. A strategic method of  $\mu$ CT 3D image segmentation of the fibers via gray level thresholding has been developed to capture efficiently the Euler orientation angles of the fibers. Avizo and Visilog softwares were used for this purpose. The second-order fiber orientation tensors have been computed based on the data of fibers' Euler angles. The normalized first tensor components ( $a_{11}$ ) of the two studied  $\mu$ CT volumes are shown in Fig. 3. The  $a_{11}$  tensor component represents the degree of fibers to orient longitudinal (parallel) with respect to the MFD. Higher value of  $a_{11}$  constitutes higher tendency of fibers to orient to the MFD. It can be seen from Fig. 3 that the skin-shell-core layers of the two  $\mu$ CT samples are well-defined. In addition, small transition regions between the shell and core layers are also observed.

Based on the qualitative and quantitative analysis by  $\mu$ CT, it can be seen that the skin layers, the upper and lower specimen surfaces, are slightly random in fiber orientation. However, the orientation tensor (Fig. 3) shows that the principal fiber orientation in the skin layer tends to follow the MFD. The shell layers are the most dominant ones with preferential fiber orientation longitudinal to the MFD. Thin core layer is developed and mostly fibers in this layer are oriented transversely to the MFD. It is worth noting that instead of purely oriented transversely to the MFD, it has been frequently observed that fibers in the core layer are slightly tilted around 5–20° from the transverse direction, such as the one shown in Fig. 2d. In addition to the skin, shell and core microstructures, transition layers between shell and core are also observed, as shown in Figs. 2c and 3.

The normalized orientation tensors of the two studied samples show that both positions exhibit almost the same state of fiber orientations. Only small differences on the width of the shell-core transition zones and the orientation state of the skin layers are observed between the two studied samples. It can be inferred from the results that the microstructure developed along the MFD axis of the injection molding plate is generally homogeneous.

## 3. Specimen

Specimens used for mechanical tests were machined from the rectangular plate produced by injection molding. To consider the

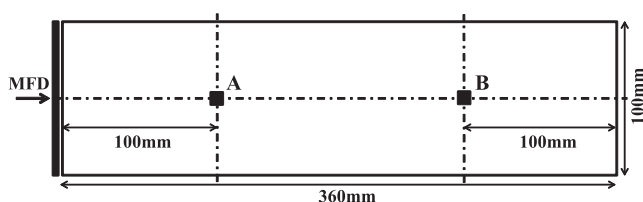


Fig. 1. Locations of  $\mu$ CT sample extraction for injection molding induced microstructure investigation (A and B).

Download English Version:

<https://daneshyari.com/en/article/817697>

Download Persian Version:

<https://daneshyari.com/article/817697>

[Daneshyari.com](https://daneshyari.com)